rhombically distorted situation. Finally, it is noteworthy that the small negative J value deduced from the susceptibility data does not markedly attenuate the Mössbauer hyperfine splitting, as it does in more strongly antiferromagnetically coupled molecules of the types $[Fe(acac)_2Cl]$[5,28] and $[Fe(salen)_2Cl]$.[31] Large hyperfine splittings were also observed for the very weakly coupled complexes [Fe(TPP)Cl],[30] [Fe(OEP)Cl],[30] and $[Fe(pyrrolidyl\text{-}dtc)_3]$.[34]

Acknowledgment. The Mössbauer spectra were obtained during a period of study leave at the University of Liverpool by P.E.C.; the hospitality of the Physics Department and useful discussions with C. D. Johnson and J. D. Rush are gratefully acknowledged. Grants from the Australian Research Grants Scheme (to K.S.M. and A.H.W.) and Monash University Special Research Grants (to K.S.M.) are gratefully acknowledged. We are grateful to Dr. P. J. Newman for providing the crystals of the iron complex and to Dr. J. R. Pilbrow for access to the ESR spectrometer.

Registry No. I, 87371-98-0.

Supplementary Material Available: Least-squares planes (Table V), non-hydrogen anisotropic thermal parameters (Table VI), atomic fractional cell and isotropic thermal parameters (hydrogen atoms) (Table VII), hydrogen atom geometries (Table VIII), structure factor amplitudes (Table IX), temperature-dependent magnetic susceptibility data (Table X), and the unit cell projected down b (Figure 7) (17 pages). Ordering information is given on any current masthead page.

(34) Rickards, R.; Johnson, C. E.; Hill, H. A. O. *J. Chem. Phys.* **1969**, *51*, 846.

Contribution from the Department of Chemistry and Biochemistry and Molecular Biology Institute, University of California, Los Angeles, California 90024

Crystal Structure and Properties of a Potassium Cryptate Salt of Bis(4-methylimidazolato)(tetraphenylporphinato)iron(III)

ROBERT QUINN, CHARLES E. STROUSE, and JOAN S. VALENTINE*

Received September 13, 1982

The synthesis and characterization of the potassium cryptate salt of bis(4-methylimidazolato)(tetraphenylporphinato)iron(III) (**1**) are reported. The salt crystallizes as the toluene solvate, $C_{77}FeH_{82}KN_{10}O_6$, in the triclinic space group $P\bar{1}$ with 2 formula units in the unit cell. At 117 K, the unit cell parameters are a = 14.63 (1) Å, b = 14.68 (1) Å, c = 17.20 (1) Å, α = 93.67 (7)°, β = 87.44 (7)°, and γ = 109.69 (7)°. The structure was solved with 3655 observed reflections, and refinement led to conventional and weighted R values of 10.7 and 10.1. The mean Fe–N(porphyrin) bond length, 1.998 (25) Å, is consistent with those of other low-spin ferric porphyrin complexes. The Fe–N(ligand) bond lengths are 1.928 (12) and 1.958 (12) Å. A comparison with Fe–N(ligand) bond lengths of $[FeTPP(ImH)_2]Cl$ (TPP = tetraphenylporphyrin; ImH = imidazole) indicates that deprotonation of imidazole may result in a 0.06-Å shortening of the axial bond lengths. Visible and EPR spectral results are consistent with the presence of a low-spin, six-coordinate ferric porphyrin complex in dimethylacetamide solution and in the solid. A comparison of the results of cyclic voltammetry of **1** and its protonated analogue, $[FeTPP(4MeImH)_2]SbF_6$ (4MeImH = 4-methylimidazole), indicates that reduction of the imidazolate complex occurs at a potential that is 700 mV more negative than that of the imidazole complex.

Introduction

Imidazolate complexes of iron porphyrins have been synthesized and studied recently[1-13] in the hope that their properties may provide information concerning the effect of deprotonation or strong hydrogen bonding of the axial histidyl imidazole ligand on the properties of certain hemoproteins. For at least one such protein, horseradish peroxidase (HRP), NMR evidence indicates that the axial histidyl imidazole is not totally deprotonated.[14] However, the possibility remains that some of the properties of HRP that are unusual when compared to hemoglobin or myoglobin,[14,15] for example, may be accounted for by a coordinated imidazole strongly hydrogen bonded to a protein residue or the protein backbone.[1] A survey of crystallographically characterized hemoproteins indicates that such hydrogen bonding is a common feature of these proteins.[16] Imidazolate is a model for the extreme case of a strongly hydrogen-bonded imidazole and thus information concerning imidazolate complexes of iron porphyrins may prove useful in understanding properties of hemoproteins in general as well as the case of any hemoprotein that may be

(1) Quinn, R.; Nappa, M.; Valentine, J. S. *J. Am. Chem. Soc.* **1982**, *104*, 2588-2595.
(2) Nappa, M.; Valentine, J. S.; Synder, P. A. *J. Am. Chem. Soc.* **1977**, *99*, 5799-5800.
(3) Landrum, J. T.; Hatano, K.; Scheidt, W. R.; Reed, C. A. *J. Am. Chem. Soc.* **1980**, *102*, 6729-6735.
(4) Landrum, J. T.; Grimmett, D.; Haller, K. J.; Scheidt, W. R.; Reed, C. A. *J. Am. Chem. Soc.* **1981**, *103*, 2640-2650.
(5) Peisach, J.; Mims, W. B. *Biochemistry* **1977**, *16*, 2795-2799.
(6) Peisach, J.; Blumberg, W. E.; Adler, A. *Ann. N.Y. Acad. Sci.* **1973**, *206*, 310-327.
(7) Cohen, I. A.; Ostfeld, D. *ACS Symp. Ser.* **1974**, *No. 5*, 221-233.
(8) Swartz, J. C.; Stanford, M. A.; Moy, J. N.; Hoffman, B. M.; Valentine, J. S. *J. Am. Chem. Soc.* **1979**, *101*, 3396-3398.
(9) Stanford, M. A.; Swartz, J. C.; Phillips, T. E.; Hoffman, B. M. *J. Am. Chem. Soc.* **1980**, *102*, 4492-4499.
(10) Stein, P.; Mitchell, M.; Spiro, T. G. *J. Am. Chem. Soc.* **1980**, *102*, 7795-7797.
(11) Mincey, T.; Traylor, T. G. *J. Am. Chem. Soc.* **1979**, *101*, 765-766.
(12) Chacko, V. P.; La Mar, G. N. *J. Am. Chem. Soc.* **1982**, *104*, 7002-7007.
(13) Stong, J. D.; Burke, J. M.; Daly, P.; Wright, P.; Spiro, T. G. *J. Am. Chem. Soc.* **1980**, *102*, 5815-5819.
(14) La Mar, G. N.; de Ropp, J. S. *Biochem. Biophys. Res. Commun.* **1979**, *90*, 36-41.
(15) Kobayashi, K.; Tamura, M.; Hayashi, K.; Hori, H.; Morimoto, H. *J. Biol. Chem.* **1980**, *255*, 2239-2242.
(16) Valentine, J. S.; Sheridan, R. P.; Allen, L. C.; Kahn, P. C. *Proc. Natl. Acad. Sci. U.S.A.* **1979**, *76*, 1009-1013.

0020-1669/83/1322-3934$01.50/0

demonstrated in the future actually to contain deprotonated histidyl imidazole.

The recent efforts to elucidate the properties of imidazolate complexes of iron porphyrins have demonstrated substantial differences between ImH[17] and Im^- as ligands. Coordination of Im^- to a ferrous[3,11] or ferric[1,3,5] porphyrin results in a shift of visible absorption bands to the red relative to ImH. The ferric complexes $FeP(ImH)_2^+$ and $FeP(Im)_2^-$ both have typically low-spin EPR spectra,[1,2,6,12] but the *g* values for the Im^- complex are shifted relative to those of ImH. The larger tetragonality value for the Im^- complex, derived from EPR *g* values for the low-spin ferric complex,[18] implies that Im^- is a stronger field ligand than ImH. Determination of the rate of CO binding to $Fe^{II}P(ImH)$ and $Fe^{II}P(Im)^-$ has shown that Im^- also exerts a pronounced trans effect[8,9] relative to ImH. Studies of the ligand binding properties of ferric and ferrous complexes have shown that $Fe^{III}P(Im)$[1] and $Fe^{II}P(Im)^-$[11] have relatively low ligand affinities compared to their protonated analogues.

Numerous imidazole complexes of ferric porphyrins have been characterized. Such complexes have generally been synthesized by reaction of FePX with imidazole or an imidazole derivative, invariably resulting in isolation of the low-spin, six-coordinate complex $[FeP(L)_2]X$. Four crystal structures of such complexes have been reported.[19-22] By contrast, the analogous imidazolate complexes are difficult to isolate and consequently are less well characterized. As in the case of ImH, Im^- complexes of ferric porphyrins have been generated by reaction of FePX with excess imidazolate[1-3] and the resulting solution species[1,2] have been shown to be six-coordinate and low spin. Isolation of monomeric Im^- complexes has proven to be difficult, however, due to the bidentate nature of Im^- and has led to imidazolate-bridged polymeric species[1,2,7] which are usually difficult to crystallize. Only three monomeric ferric porphyrin imidazolate complexes have been isolated: a five-coordinate complex of a highly sterically hindered Im^-[3] and two low-spin, six-coordinate complexes, $(Bu_4N)[FeTPP(Im)_2]$[3] and $[K(18C6)][FeTPP(4MeIm)_2]$.[1] No crystal structures of mononuclear Im^- complexes of ferric porphyrins have been obtained prior to this study and the only published structure of a metalloporphyrin imidazolate complex is that of $[MnTPP(Im)]_n$, a polymeric species.[3]

Our earlier attempts at isolation of monomeric imidazolate complexes involved reaction of Fe(TPP)Cl with K(Im) solubilized with crown ether. But isolation of the reaction product resulted in a polymeric product, $[FeTPP(Im)]_n$.[2,7] It soon became apparent that steric bulk on either the porphyrin or the ligand was necessary to inhibit the close approach of two iron centers. The approach we chose was the use of a ligand with a bulky substituent, i.e., $4MeIm^-$. This ligand forms a sterically unhindered bond to a ferric porphyrin, but the presence of the methyl group at the four position inhibits coordination to a second iron center, permitting isolation of a monomeric complex. Previously we have shown that reaction of Fe(TPP)Cl with K(4MeIm) solubilized with 18C6 resulted in isolation of the low-spin complex, $[K(18C6)][FeTPP(4MeIm)_2]$.[1] Recently we have found that substitution of K222 for 18C6 resulted in an analogous complex for which crystals suitable for crystallography were obtained. Herein, we report the first crystal and molecular structure and properties of a ferric porphyrin imidazolate complex, $[K(K222)][FeTPP(4MeIm)_2]\cdot C_7H_8$.

Table I. Experimental Parameters

formula	$C_{77}FeH_{82}KN_{10}O_6$
Z	2
color	black
habit	parallelepiped
a	14.63 (1) Å
b	14.68 (1) Å
c	17.20 (1) Å
α	93.67 (7)°
β	87.44 (7)°
γ	109.69 (7)°
wavelength	0.71069 Å
temp	117 K
radiation	Mo K (crystal monochromatized)
space group	$P\bar{1}$ (confirmed by successful refinement)
cryst dimens	0.09 × 0.45 × 0.52 mm
abs coeff	3.34 cm^{-1}
transmission factors	$T(min) = 0.87$; $T(max) = 0.97$ (analytical)
diffractometer	Syntex $P\bar{1}$
geometry	$\theta/2\theta$
$2\theta(max)$	45°
data collected	$\pm h, \pm k, \pm l$
no. of data measd	9121
no. of indep data	9121
no. of data obsd with $[I > 2\sigma(I)]$	3655
R	0.107
R_w	0.101

Experimental Section

General Methods. All reactions and distillations were carried out under an inert atmosphere (He or Ar) with use of Schlenkware or a Vacuum Atmospheres inert-atmosphere chamber. All materials and glassware were thoroughly dried in order to protect against formation of $(FeTPP)_2O$.

Materials. DMA was distilled from CaH_2 under reduced pressure. CH_2Cl_2 was distilled from CaH_2. Toluene and THF were distilled from Na/benzophenone. All solvents were stored over molecular sieves. Fe(TPP)Cl, $FeTPP(SbF_6)$, K(4MeIm), and 4MeImH were prepared and/or purified as described previously.[1] 1MeIm was vacuum distilled from CaH_2 and stored over molecular sieves. K222 and TBAP were dried over P_2O_5 in vacuo prior to use. $FeTPP(4MeImH)_2SbF_6$ was synthesized by reaction of 2 mM $FeTPP(SbF_6)$ in toluene with 2 equiv of 4MeImH. The solid product was collected by filtration, washed with toluene, recrystallized from CH_2Cl_2/toluene, and dried in vacuo. $FeTPP(1MeIm)_2SbF_6$ was synthesized and purified in an identical manner.

Synthesis of $[K(K222)][FeTPP(4MeIm)_2]$ (1). To a 2.2 mM solution of Fe(TPP)Cl in toluene was added an equal volume of toluene containing 3.9 equiv of K(4MeIm) and 9.0 equiv of K222. The mixture was stirred for 4 h and then filtered. The resulting purple solid was washed with toluene and dissolved in DMA, yielding a 6.3 mM solution. Toluene was added until the porphyrin concentration was 1.3 mM. After the mixture was allowed to stand for several days at room temperature, crystals of crystallographic quality had formed. A sample for elemental analysis was separated by filtration and washed with toluene. Anal. Calcd for $[K(K222)][FeTPP(4MeIm)_2]\cdot C_7H_8$, $C_{77}H_{82}N_{10}O_6FeK$: C, 69.9; H, 6.18; N, 10.46; K, 2.92. Found: C, 66.96; H, 6.01; N, 10.74; K, 3.3. An IR spectrum in KBr revealed no bands in the 4000–32000-cm^{-1} region, confirming that the ligands were deprotonated.

Methods. Cyclic voltammograms were recorded by using a Bioanalytical Systems Model CV-1B-120 apparatus, a Houston XY recorder, and a three-electrode system consisting of a Pt-button working

(17) Abbreviations used in this paper are as follows: ImH, imidazole; Im^-, imidazolate; 4MeImH, 4-methylimidazole; $4MeIm^-$, 4-methylimidazolate; P, porphyrin; TPP, tetraphenylporphyrin; Bu_4N^+, tetrabutylammonium ion; 18C6, 18-crown-6, 1,4,7,10,13,16-hexaoxacyclooctadecane; K222, Kryptofix 222, 4,7,13,16,21,24-hexaoxa-1,10-diazabicyclo[8.8.8]hexacosane; DMA, dimethylacetamide; THF, tetrahydrofuran; 1MeIm, 1-methylimidazole; TBAP, tetrabutylammonium perchlorate; py, pyridine; SPh^-, benzenethiolate; PPIX, protoporphyrin IX; OEP, octaethylporphyrin; $2MeIm^-$, 2-methylimidazolate; DMF, dimethylformamide; Me_2SO, dimethyl sulfoxide; sh, shoulder.

(18) Taylor, C. P. S. *Biochim. Biophys. Acta* **1977**, *491*, 137–148.
(19) Collins, D. M.; Countryman, R.; Hoard, J. L. *J. Am. Chem. Soc.* **1972**, *94*, 2066–2072.
(20) Little, R. G.; Dymock, K. R.; Ibers, J. A. *J. Am. Chem. Soc.* **1975**, *97*, 4532–4539.
(21) Takenaka, A.; Sasada, Y.; Watanabe, E.; Ogoshi, H.; Yoshida, Z. *Chem. Lett.* **1972**, 1235–1238.
(22) Kirner, J. F.; Hoard, J. L.; Reed, C. A. "Abstracts of Papers", 175th National Meeting of the American Chemical Society, Anaheim, CA, March 13–17, 1978; American Chemical Society; Washington, DC, 1978; INOR 14.

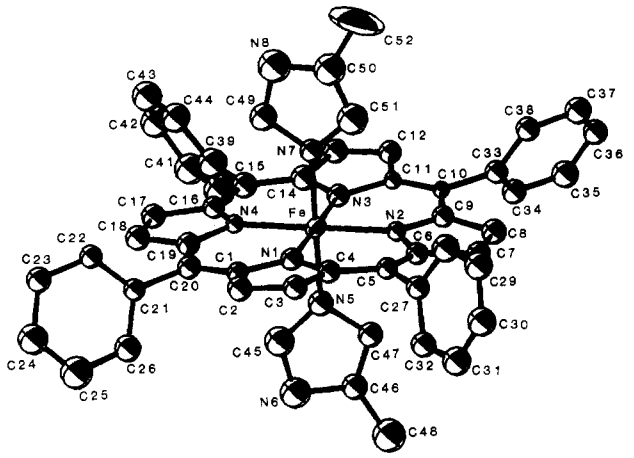

Figure 1. ORTEP plot of [K(K222)][FeTPP(4MeIm)$_2$] showing the anionic complex only and its numbering scheme. 4MeIm$_a^-$ is located below the porphyrin plane; 4MeIm$_b^-$ above. Hydrogen atoms have been omitted for clarity.

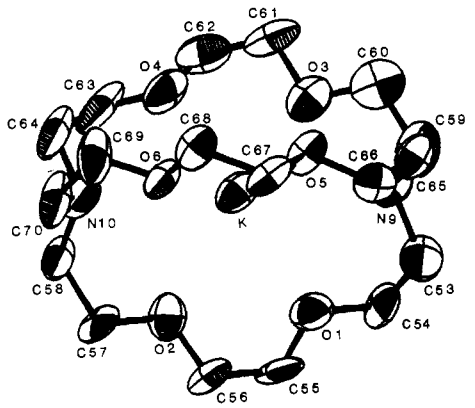

Figure 2. ORTEP plot of the potassium cryptate cation showing the numbering scheme. Hydrogen atoms have been omitted for clarity.

electrode, a Pt-wire auxiliary electrode, and a saturated calomel (SCE) reference electrode. To inhibit contamination with water, the reference electrode was separated by using an electrode bridge tube fitted with a Vycor tip. All data were collected in DMA with 0.1 M TBAP supporting electrolyte. The solvent and supporting electrolyte were stable between +1.0 and −2.0 V. Typically, porphyrin concentrations were 1 mM, and the scan speed was 50 mV/s.

Visible spectra were recorded as described previously.[1] EPR spectra were recorded on a Varian E-12 apparatus and calibrated with DPPH and a Gauss meter.

X-ray Structure Determination. A summary of crystallographic parameters is given in Table I. All data analysis made use of the UCLA Crystallographic Computing Package. Scattering factors and anomalous dispersion corrections were taken from ref 23.

Analytical, difference Fourier, and least-squares refinement techniques were used to locate all non-hydrogen atoms in the structure. Positions of many hydrogens were located in a difference map. The final positions of all hydrogens were calculated by using idealized bond distances and their positions were held constant during subsequent refinements. Positions of all non-hydrogen atoms were refined, along with anisotropic thermal parameters of Fe, C(52), and all atoms of the toluene solvate and the potassium cryptate cation. A final least-squares refinement led to $R = 10.7$, $R_w = 10.1$, an error of fit of 2.24, and a data to parameter ratio of 6.8. The relatively high R value reflects the poor quality and large mosaicity of the crystal that appeared to result from rapid solvate loss during crystal mounting. Numerous attempts to obtain a better quality crystal were unsucessful.

Results and Discussion

Crystal Structure. The structure of the anionic complex and the numbering scheme used are illustrated in Figure 1. The structure of the potassium cryptate cation and its numbering scheme are illustrated in Figure 2. Atomic coordinates are listed in Table II. Perpendicular displacements in units of 0.01 Å from the least-squares plane of the 24 core atoms are illustrated in Figure 3. Displacements are in accord with those for other TPP derivatives.[19] The porphyrinato core displays approximate D_{2d} symmetry.

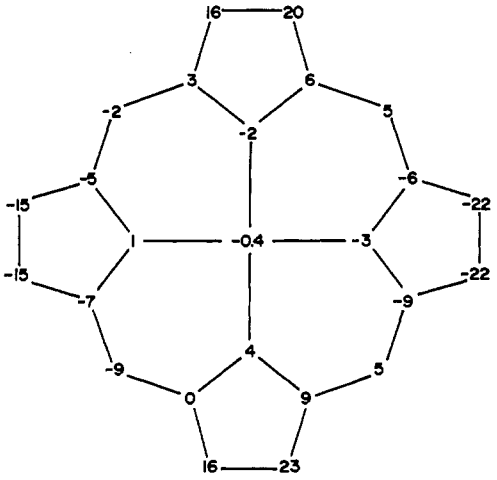

Figure 3. Displacements in units of 0.01 Å from the mean plane of the 24-atom porphyrin core. The porphyrin is oriented as in Figure 1.

Selected bond lengths and angles for the porphyrin core and axial ligand atoms are reported in Tables III and IV. Selected bond lengths of the potassium cryptate cation are listed in Table V. The Fe–N(porphyrin) bond lengths are in accord with those expected for a low-spin ferric porphyrin. Although considerable variation in the individual Fe–N(p) bond lengths is observed, the average Fe–N(p) bond length of 1.998 (25) Å[24] is not significantly different from that of FeTPP(ImH)$_2$Cl,[19] 1.989 (8), or those of two anionic, low-spin ferric complexes, 2.009 (8) Å for FeTPP(SPh)$_2^-$[25] and 2.000 (6) Å for FeTPP(CN)$_2^-$.[26] Further, this value is consistent with 1.990 Å, the average of Fe–N(p) bond distances for an extensive tabulation of low-spin ferric porphyrin structures.[27] Average bond lengths of **1** and those of FeTPP(ImH)$_2$Cl for comparison are listed in Table VI.

Fe–N(Im$^-$) bond lengths are 1.928 (12) and 1.958 (12) Å for 4MeIm$_a^-$ and 4MeIm$_b^-$, respectively. This difference is not statistically significant. Both imidazolate rings are essentially perpendicular to the porphyrin plane with mean ligand plane to mean porphyrin plane angles of 88.2° for 4MeIm$_a^-$ and 91.2° for 4MeIm$_b^-$. The average N(Im$^-$)–Fe–N(p) angles are 90.1 and 90.2°, respectively, and the N(5)–Fe–N(7) angle is 179.4 (6)°. Both imidazolate rings are planar with the five aromatic atoms displaced less than 0.01 Å from the mean ligand plane.

Comparisons between Fe–N(Im$^-$) and Fe–N(ImH) distances must take into account the fact that the principal determinant of Fe–imidazole bond lengths is steric interactions between porphyrin and ligand atoms. The orientation of planar ligands relative to the porphyrin plane has been described by Collins et al.[19] in terms of an angle, ϕ, between an N(p)–Fe–N(p) axis and the projection of the ligand plane on the porphyrin plane. Steric interactions between ligand H atoms

(23) "International Tables for X-ray Crystallography"; Kynoch Press: Birmingham, England, 1974.

(24) For average values, numbers in parentheses are estimated standard deviations of the average on the assumption that the values averaged are drawn from the same population.

(25) Byrn, M. P.; Strouse, C. E. *J. Am. Chem. Soc.* **1981**, *103*, 2633–2635.

(26) Scheidt, W. R.; Haller, K. J.; Hatano, K. *J. Am. Chem. Soc.* **1980**, *102*, 3017–3021.

(27) Scheidt, W. R.; Reed, C. A. *Chem. Rev.* **1981**, *81*, 543–555.

Table II. Atomic Coordinates in the Unit Cell[a]

atom	x	y	z	atom	x	y	z
Fe	0.6470 (2)	0.2840 (2)	0.2341 (1)	C(39)	0.6915 (12)	0.6105 (12)	0.1475 (10)
N(1)	0.5678 (8)	0.2022 (8)	0.3204 (7)	C(40)	0.6651 (12)	0.6232 (12)	0.0734 (10)
N(2)	0.7023 (8)	0.1821 (8)	0.2000 (6)	C(41)	0.6819 (12)	0.7188 (12)	0.0514 (9)
N(3)	0.7259 (8)	0.3664 (8)	0.1500 (7)	C(42)	0.7232 (12)	0.7937 (11)	0.1052 (10)
N(4)	0.5922 (8)	0.3874 (7)	0.2667 (6)	C(43)	0.7468 (12)	0.7834 (12)	0.1774 (10)
N(5)	0.5427 (9)	0.2290 (8)	0.1622 (7)	C(44)	0.7293 (11)	0.6882 (12)	0.1998 (9)
N(6)	0.3936 (10)	0.1898 (9)	0.1047 (8)	C(45)	0.4547 (13)	0.2411 (11)	0.1589 (10)
N(7)	0.7537 (8)	0.3391 (8)	0.3064 (7)	C(46)	0.4499 (11)	0.1395 (11)	0.0662 (9)
N(8)	0.8473 (11)	0.4382 (10)	0.4007 (8)	C(47)	0.5373 (11)	0.1607 (10)	0.0991 (9)
C(1)	0.5017 (10)	0.2237 (10)	0.3712 (8)	C(48)	0.4072 (13)	0.0727 (12)	−0.0007 (10)
C(2)	0.4696 (11)	0.1518 (11)	0.4254 (9)	C(49)	0.7665 (12)	0.4202 (11)	0.3552 (9)
C(3)	0.5126 (11)	0.0850 (10)	0.4050 (8)	C(50)	0.8834 (14)	0.3670 (13)	0.3775 (11)
C(4)	0.5712 (10)	0.1126 (10)	0.3368 (8)	C(51)	0.8293 (13)	0.3076 (12)	0.3215 (10)
C(5)	0.6223 (10)	0.0613 (10)	0.2965 (8)	C(52)	0.9725 (15)	0.3597 (19)	0.4183 (14)
C(6)	0.6766 (10)	0.0912 (10)	0.2317 (8)	K	0.2053 (3)	0.7045 (3)	0.2794 (2)
C(7)	0.7261 (11)	0.0333 (10)	0.1866 (9)	N(9)	0.2211 (12)	0.5194 (10)	0.2051 (9)
C(8)	0.7793 (11)	0.0879 (11)	0.1309 (9)	N(10)	0.1895 (14)	0.8930 (12)	0.3474 (12)
C(9)	0.7669 (10)	0.1808 (10)	0.1411 (8)	O(1)	0.0396 (9)	0.5522 (9)	0.2420 (7)
C(10)	0.8143 (9)	0.2595 (9)	0.0966 (7)	O(2)	0.0196 (9)	0.7305 (10)	0.2923 (7)
C(11)	0.7948 (10)	0.3459 (9)	0.1003 (8)	O(3)	0.3148 (10)	0.7041 (11)	0.1379 (7)
C(12)	0.8439 (10)	0.4276 (10)	0.0564 (8)	O(4)	0.3192 (10)	0.8791 (10)	0.2126 (11)
C(13)	0.8055 (11)	0.4980 (10)	0.0753 (9)	O(5)	0.2945 (8)	0.5984 (8)	0.3630 (6)
C(14)	0.7328 (11)	0.4597 (11)	0.1335 (9)	O(6)	0.2502 (9)	0.7589 (9)	0.4340 (7)
C(15)	0.6746 (11)	0.5083 (11)	0.1717 (9)	C(53)	0.1244 (17)	0.4422 (15)	0.2028 (12)
C(16)	0.6098 (11)	0.4730 (10)	0.2321 (8)	C(54)	0.0457 (15)	0.4789 (13)	0.1846 (11)
C(17)	0.5489 (11)	0.5242 (10)	0.2680 (9)	C(55)	−0.0495 (14)	0.5659 (14)	0.2413 (11)
C(18)	0.4955 (11)	0.4704 (11)	0.3231 (9)	C(56)	−0.0542 (13)	0.6368 (14)	0.3059 (11)
C(19)	0.5207 (11)	0.3833 (10)	0.3221 (9)	C(57)	0.0104 (13)	0.8041 (14)	0.3416 (11)
C(20)	0.4771 (11)	0.3067 (10)	0.3716 (8)	C(58)	0.0940 (15)	0.8976 (13)	0.3308 (13)
C(21)	0.3958 (11)	0.3137 (10)	0.4259 (8)	C(59)	0.2589 (18)	0.5311 (16)	0.1265 (12)
C(22)	0.4083 (10)	0.3769 (10)	0.4872 (8)	C(60)	0.3424 (16)	0.6240 (20)	0.1177 (10)
C(23)	0.3296 (11)	0.3871 (10)	0.5316 (8)	C(61)	0.3915 (15)	0.7918 (19)	0.1245 (12)
C(24)	0.2351 (12)	0.3298 (12)	0.5094 (10)	C(62)	0.3596 (17)	0.8730 (20)	0.1370 (16)
C(25)	0.2218 (13)	0.2645 (12)	0.4503 (10)	C(63)	0.2888 (18)	0.9551 (17)	0.2273 (19)
C(26)	0.3017 (12)	0.2572 (11)	0.4064 (9)	C(64)	0.2664 (19)	0.9744 (16)	0.3111 (20)
C(27)	0.6096 (11)	−0.0369 (10)	0.3231 (8)	C(65)	0.2808 (14)	0.4866 (12)	0.2539 (11)
C(28)	0.6847 (11)	−0.0547 (11)	0.3586 (9)	C(66)	0.2581 (13)	0.4967 (13)	0.3409 (11)
C(29)	0.6767 (12)	−0.1484 (11)	0.3790 (9)	C(67)	0.2761 (12)	0.6089 (12)	0.4448 (10)
C(30)	0.5926 (12)	−0.2218 (11)	0.3657 (9)	C(68)	0.3092 (14)	0.7157 (14)	0.4688 (10)
C(31)	0.5190 (12)	−0.2088 (11)	0.3303 (9)	C(69)	0.2763 (15)	0.8558 (15)	0.4568 (12)
C(32)	0.5255 (11)	−0.1146 (11)	0.3086 (8)	C(70)	0.2020 (16)	0.8957 (13)	0.4321 (14)
C(33)	0.8894 (11)	0.2480 (10)	0.0382 (9)	C(71)	1.0950 (15)	0.0626 (14)	0.1434 (12)
C(34)	0.8826 (11)	0.2588 (10)	−0.0402 (9)	C(72)	1.1558 (14)	0.1488 (14)	0.1804 (12)
C(35)	0.9536 (12)	0.2494 (11)	−0.0937 (9)	C(73)	1.1147 (18)	0.1757 (14)	0.2489 (13)
C(36)	1.0367 (11)	0.2410 (10)	−0.0674 (9)	C(74)	1.0213 (20)	0.1325 (20)	0.2757 (13)
C(37)	1.0467 (11)	0.2314 (10)	0.0113 (9)	C(75)	0.9680 (15)	0.0468 (16)	0.2362 (15)
C(38)	0.9742 (11)	0.2374 (10)	0.0654 (8)	C(76)	1.0020 (14)	0.0138 (13)	0.1682 (11)
				C(77)	1.1307 (15)	0.0275 (13)	0.0663 (12)

[a] Numbers in parentheses following atomic coordinates are estimated standard deviations.

Table III. Selected Bond Lengths (Å) of Porphyrinato Core and Ligand Atoms[a]

$Fe-N_1$	2.031 (12)	N_6-C_{46}	1.400 (17)
$Fe-N_2$	1.974 (11)	$C_{46}-C_{47}$	1.352 (18)
$Fe-N_3$	2.006 (12)	$C_{46}-C_{48}$	1.477 (20)
$Fe-N_4$	1.982 (11)	N_7-C_{49}	1.375 (16)
$Fe-N_5$	1.928 (12)	N_7-C_{51}	1.375 (17)
$Fe-N_7$	1.958 (12)	N_8-C_{49}	1.386 (18)
N_5-C_{45}	1.361 (17)	N_8-C_{50}	1.353 (18)
N_5-C_{47}	1.416 (16)	$C_{50}-C_{51}$	1.346 (20)
N_6-C_{45}	1.328 (17)	$C_{50}-C_{52}$	1.544 (25)

[a] Numbers in parentheses are estimated standard deviations.

Table IV. Selected Bond Angles (deg) of Porphyrinato Core and Ligand Atoms[a]

N_1FeN_2	91.2 (5)	FeN_4C_{19}	127.3 (10)
N_2FeN_3	89.4 (5)	FeN_5C_{45}	130.9 (11)
N_3FeN_4	89.7 (5)	FeN_5C_{47}	127.9 (11)
N_4FeN_1	89.7 (5)	FeN_7C_{49}	125.2 (11)
N_5FeN_1	91.3 (5)	FeN_7C_{51}	129.7 (11)
N_5FeN_2	90.1 (5)	$C_{45}N_5C_{47}$	101.2 (13)
N_5FeN_3	89.4 (5)	$C_{45}N_6C_{46}$	100.6 (14)
N_5FeN_4	89.7 (5)	$N_5C_{45}N_6$	118.4 (15)
N_7FeN_1	89.0 (5)	$N_5C_{47}C_{46}$	108.1 (14)
N_7FeN_2	89.3 (5)	$N_6C_{46}C_{47}$	111.8 (14)
N_7FeN_3	90.4 (5)	$N_6C_{46}C_{48}$	118.0 (14)
N_7FeN_4	90.9 (5)	$C_{47}C_{46}C_{48}$	130.3 (16)
FeN_1C_1	127.4 (10)	$C_{49}N_7C_{51}$	105.1 (13)
FeN_1C_4	124.4 (10)	$C_{49}N_8C_{50}$	104.2 (15)
FeN_2C_6	124.9 (10)	$N_7C_{49}N_8$	110.8 (14)
FeN_2C_9	129.6 (10)	$N_7C_{51}C_{50}$	108.6 (16)
FeN_3C_{11}	126.8 (9)	$N_8C_{50}C_{51}$	111.2 (17)
FeN_3C_{14}	128.7 (10)	$N_8C_{50}C_{52}$	119.7 (19)
FeN_4C_{16}	126.7 (10)	$C_{51}C_{50}C_{52}$	129.0 (19)

[a] Numbers in parentheses are estimated standard deviations.

and porphyrin pyrrole nitrogen atoms are minimized at ϕ = 45°, i.e., the position in which the ligand plane bisects adjacent pyrrole nitrogens. For ϕ < 45°, ligand H atoms and pyrrole nitrogens are closer, resulting in increased steric interactions, with ϕ = 0° yielding maximum interaction. Generally, such ligand–porphyrin nonbonding interactions are observed to be at distances of 2.50 Å or greater.[28] $FeTPP(ImH)_2Cl$ has ligands at ϕ = 39 and 18° with H(ImH)···N(p) distances of 2.79 (ImH_a) and 2.56–2.58 Å (ImH_b), respectively.[19] The

(28) Cullen, D. L.; Meyer, E. F. *Acta Crystallogr., Sect. B* **1976**, *B32*, 2259–2269.

Table V. Selected and Average Bond Lengths (Å) of the Potassium Cryptate Cation[a]

	Selected		
$K-O_1$	2.756 (13)	$K-O_4$	2.827 (14)
$K-O_2$	2.866 (13)	$K-O_5$	2.832 (11)
$K-O_3$	2.852 (14)	$K-O_6$	2.770 (13)
	Average		
K-O	2.82 (4)[b]	O-C	1.41 (3)
C-C	1.49 (3)	N-C	1.47 (2)

[a] Numbers in parentheses are estimated standard deviations. [b] For average values, numbers in parentheses are estimated standard deviations of the average calculated on the assumption that the values averaged are drawn from the same population.

Table VI. Mean Bond Lengths of [K(K222)][FeTPP(4MeIm)$_2$] Compared Those of to FeTPP(ImH)$_2$Cl (Å)[a,b]

	$FeTPP(4MeIm)_2^-$	$FeTPP(ImH)_2^+$
Fe-N(p)	1.998 (25)[c]	1.989 (8)
Fe-N(L)	1.943 (21)	1.974 (24)
C(a)-N(p)	1.379 (13)	1.378 (10)
C(a)-C(b)	1.430 (19)	1.437 (12)
C(b)-C(b)	1.340 (16)	1.350 (9)
C(a)-C(m)	1.383 (19)	1.392 (11)
C(m)-C(ph)	1.504 (12)	1.498 (13)
C(ph)-C(ph)	1.38 (3)	1.38 (2)

[a] Reference 19. [b] N(p) and N(L) are porphyrin and ligand nitrogens, respectively. C(a) and C(b) are carbons at α and β pyrrole positions, respectively. C(m) are methine carbons, and C(ph) are phenyl carbons. [c] Numbers in parentheses are estimated standard deviations of the average calculated on the assumption that the values averaged are drawn from the same population.

ligand at 39° suffers less steric interaction, resulting in a shorter Fe–N(L) bond length, 1.957 (4) Å, than the ligand at 18°, 1.991 (5) Å. Similarly, for Fe^{III}PPIX(1MeIm)$_2$,[20] 1MeIm at ϕ = 16° leads to a bond length of 1.966 (5) Å, shorter than 1MeIm at ϕ = 3°, 1.988 (5) Å. FeOEP(ImH)$_2$ClO$_4$ has ImH arranged in a coplanar fashion with ϕ = 7° and axial bond distances of 2.01 (2) Å for both, as required by molecular symmetry.[21]

In the present structure, the ligands are oriented at nonequivalent dihedral angles of ϕ = 17° for $4MeIm_a^-$ and ϕ = 1° for $4MeIm_b^-$, as illustrated in Figure 4. The angle between the mean ligand planes is 18°. The closest contacts between the H(4MeIm$^-$) and N(pyrrole) atoms are as follows: for $4MeIm_a^-$, H(45)···N(4) = 2.54 Å and H(47)···N(2) = 2.59 Å; for $4MeIm_b^-$, H(49)···N(4) = 2.43 Å and H(51)···N(2) = 2.57 Å. Other interactions at distances of 2.90 Å or less occur between H(ligand) and C(α) atoms and are as follows: for $4MeIm_a^-$, H(45)···C(19) = 2.58 Å; for $4MeIm_b^-$, H(49)···C(19) = 2.87 Å and H(51)···C(9) = 2.90 Å. The nonequivalent orientation of the ligands leads one to expect nonequivalent axial bond distances, on the basis of the previously described structures. For this reason, comparison of metal–ligand distances in different complexes should be based on

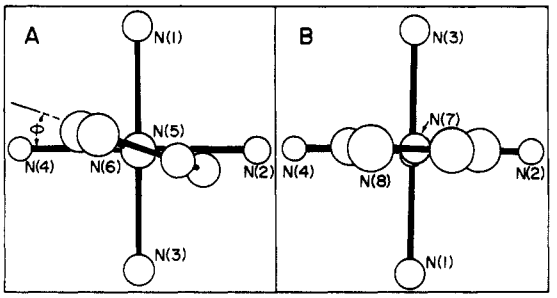

Figure 4. Orientation of axial ligands relative to N(p)–Fe–N(p) axes (methyl carbons of the ligands omitted for clarity): (A) view along the N_5–Fe axis showing the plane of $4MeIm_a^-$ (ϕ = 17°; $4MeIm_b^-$ omitted for clarity); (B) view along the N_7–Fe axis showing the plane of $4MeIm_b^-$ (ϕ = 1°; $4MeIm_a^-$ omitted for clarity).

ligands in approximately the same steric environment. $4MeIm_a^-$ in our structure of **1** and ImH_b in that of FeTPP(ImH)$_2$Cl[19] are oriented at ϕ = 17 and 18°, respectively, and have approximately the same H(ligand)–N(porphyrin) interaction distances. Hence, the steric interactions of these ligands with the porphyrin should be approximately the same. We observe, however, that the axial bond length to $4MeIm^-$ is 0.06 Å shorter than that to ImH. This difference in the Fe–Im$^-$ and Fe–ImH distances probably represents an inherent difference between ferric–imidazolate and ferric–imidazole bonding. Unfortunately, the estimated standard deviation of 0.012 Å for the Fe–N distance in the present structure determination limits the significance of this observation.

Visible and EPR Spectral Properties. In addition to crystal structure studies, we have also continued our solution characterization of **1**. We find that **1** is highly soluble in DMA (>7 mM) and at 1 mM leads to a typical low-spin ferric porphyrin visible spectrum:[1] 425 nm (Soret), 442 (sh), 558 (β), 598 (α). Compared to its protonated analogue, FeTP(4MeImH)$_2$SbF$_6$, complex **1** shows visible absorption bands significantly shifted to the red (see Table VII). That **1** is present in a 1 mM DMA solution as the six-coordinate complex only is shown by the fact that addition of 40 equiv of $4MeIm^-$ to a 1 mM solution of **1** causes no change in the visible spectrum. The presence of excess $4MeIm^-$ apparently leads to no change in the coordination state of iron.

Dilution of a DMA solution of **1** to 10^{-5} or 2×10^{-6} M results in slight but significant visible spectral changes consistent with ligand dissociation and formation of small amounts of FeTPP(4MeIm). Attempts to confirm the presence of this species by titration with excess $4MeIm^-$ leads, at 10^{-5} M Fe, to the appearance of visible bands due to a ferrous product rather than more **1** (see Table VII). The similarity of this spectrum to that of [Fe^{II}TPP(2MeIm)]$^-$ in THF[3] suggests that the analogous five-coordinate comples, [Fe^{II}TPP(4MeIm)]$^-$, is formed. The reduction of ferric porphyrins in the presence of excess ligand is not unprecedented. It has been demonstrated that piperidine and CN^- act as one-electron-reducing

Table VII. Visible Spectral Properties of [K(K222)][FeTPP(4MeIm)$_2$] and Related Species

complex or conditions	[porphyrin], mM	solvent	vis band max, nm			
1	satd	toluene	417 (10.3)[a]		576 (1.0)	624 (sh)[c] (0.67)
1	1.0	DMA	425 (12.6)	442 (sh) (8.7)	558 (1.0)	598 (0.63)
1 + 40 mM $4MeIm^-$	1.0	DMA	425 (11.8)	442 (sh) (8.4)	558 (1.0)	598 (0.62)
1	0.01	DMA	424 (12.7)	442 (sh) (8.5)	559 (1.0)	601 (sh) (0.63)
1	0.002	DMA	421 (11.9)	442 (sh) (6.3)	566 (1.0)	613 (sh) (0.45)
1 + 2 mM $4MeIm^-$	0.01	DMA	428 (11.1)	443 (12.7)	567 (1.0)	615 (0.63)
Fe^{II}TPP(2MeIm)$^-$ [b]		THF	446 (6.5)	530 (0.41)	573 (1.0)	614 (0.88)
2	1.0	DMA	416 (13.4)	458 (sh) (1.8)	544 (1.0)	578 (sh) (0.54)

[a] Numbers in parentheses are relative absorbances calculated by dividing absorbance at a particular wavelength by the absorbance at the β band. [b] Data taken from ref 3. [c] sh = shoulder.

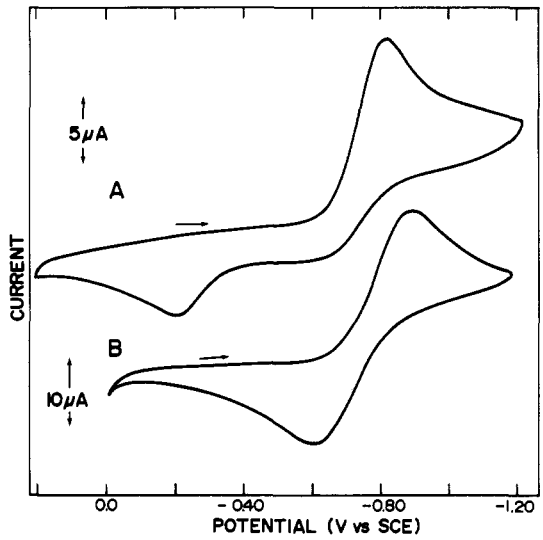

Figure 5. Cyclic voltammograms of 1 mM [K(K222)][FeTPP-(4MeIm)$_2$] (0.1 M TBAP in DMA): A, no K(4MeIm); B, 40 mM K(4MeIm).

agents and, in the case of piperidine, the rate of porphyrin reduction is increased by deprotonation of the ligand.[29] Hence, it is reasonable that excess $4MeIm^-$ leads to porphyrin reduction as well.

Dissolution of **1** in toluene leads to very different results. The complex **1** is not highly soluble in toluene, and saturated solutions, ~0.02 mM, result in Soret, β, and α bands at 417, 576, and 624 nm (sh). We have previously shown that this spectrum is due to a five-coordinate high-spin complex, FeTPP(4MeIm), which results from dissociation of **1** forming equimolar quantities of FeTPP(4MeIm) and [K(K222)]-4MeIm.[1]

The EPR spectrum of **1** is characteristic of a low-spin ferric porphyrin complex. Polycrystalline **1** at 77 K yields a major set of g values at 2.60, 2.24, and 1.82 and a minor set at 2.68 and 1.78 of unknown origin. Apparently, the third g value of the minor set is buried under the g = 2.24 signal. Solutions of **1**, 2 mM in DMA, result in g values of 2.60, 2.24, and 1.82, identical with the major g values of polycrystalline **1** and almost identical with those of $FeTPP(4MeIm)_2^-$ generated by reaction of 2 mM $FeTPP(SbF_6)$ with 30 equiv of K(4MeIm): g = 2.59, 2.24, and 1.82. In none of the above samples are high-spin ferric signals at g = 6 observed, suggesting that **1** exists as a six-coordinate complex even in the absence of excess ligand.

Cyclic Voltammetry. The cyclic voltammogram (CV) of a 1 mM solution of **1** in the presence of 40 mM $4MeIm^-$ indicates the presence of one reducible, E_{pc} = −0.88 V, and one reoxidizable species, E_{pa} = −0.64 V (see Figure 5). These are presumably **1** and $Fe^{II}TPP(4MeIm)_2^{2-}$, respectively. In the absence of added $4MeIm^-$, by contrast, an additional reoxidizable species is observed with an anodic peak at −0.20 V. The cathodic peak is also slightly shifted to −0.82 V, and there is a decrease in the current due to the anodic peak at −0.64 V. These results suggest that reduction of **1** to the ferrous complex is followed by partial ligand dissociation, resulting in an equilibrium mixture of five- and six-coordinate species, as in Scheme I. We have previously shown that $Fe^{III}TPP(4MeIm)$ has a relatively low affinity for a sixth ligand.[1] One would expect, in view of the increased electron density at the iron center, that $Fe^{II}TPP(4MeIm)^-$ would have a still lower ligand affinity. It is, therefore, not surprising that $Fe^{II}TPP(4MeIm)_2^{2-}$ undergoes partial ligand dissociation.

Scheme I[a]

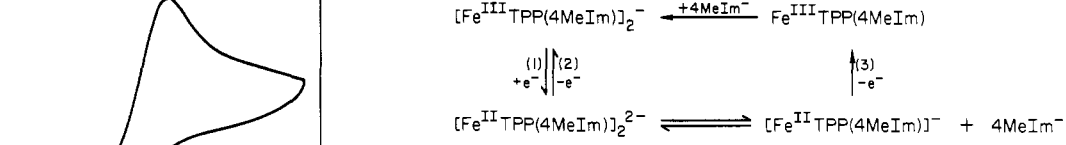

[a] Numbers in parentheses on the arrows refer to processes described in the text.

Hence, in the absence of excess ligand, reoxidation via both $Fe^{II}TPP(4MeIm)^-$, pathway 3 (E_{pa} = −0.20 V), and $Fe^{II}TPP(4MeIm)_2^{2-}$, pathway 2 (E_{pa} = −0.64 V), occurs (see Scheme I). Excess ligand shifts the equilibrium toward the fully ligated ferrous complex, and subsequent reoxidation occurs via (2), E_{pa} = −0.64 V, only. Similar results have been reported for an $Fe^{III}P(OR)$ complex;[30] in the absence of excess OR^-, two anodic peaks were observed, presumably corresponding to reoxidation of $Fe^{II}P(OR)$ and $Fe^{II}P$. Excess OR^- resulted in conversion to all $Fe^{II}P(OR)$ and only one anodic peak corresponding to reoxidation.

Although the Fe(III)/Fe(II) couple in the presence of excess ligand is not strictly reversible, the value of $^1/_2(E_{pc} + E_{pa})$ = −0.75 V for $Fe^{III}TPP(4MeIm)_2^-$ can be compared to the half-wave potential of −1.10 V for $Fe(TPP)F_2^-$ in Me_2SO.[31] To the best of our knowledge, this latter value is the only previously reported $E_{1/2}$ value for an anionic $Fe^{III}TPP$ complex. The substantially less negative potential of $FeTPP(4MeIm)_2^-$ presumably reflects reduced σ-donor and/or increased π-acceptor character of $4MeIm^-$ as compared to F^-.

Analogous CV experiments with $FeTPP(4MeImH)_2SbF_6$ (**2**) suggest that deprotonation of coordinated 4MeImH has a substantial effect not only on the value of $E_{1/2}$ for the Fe(III)/Fe(II) couple but also on the coordination state of the ferrous complex. The CV of 1 mM **2** in DMA indicates that electron transfer is reversible and gives a half-wave potential of −0.05 V for the Fe(III)/Fe(II) couple. Addition of 0.1 M 4MeImH to the above solution results in a small but significant negative shift in the half-wave potential to −0.08 V. This may be compared to $E_{1/2}$ = −0.115 V for $FeTPP(ImH)_2Cl$ in DMF with excess ImH.[32] Ligand-concentration-dependent shifts of half-wave potentials have been reported for $FeOEP(ClO_4)$ in the presence of varying pyridine concentrations where an increase in the bulk [py] from 1 to 10 mM resulted in a 126-mV negative shift in $E_{1/2}$ values.[33] This shift has been ascribed to differences in the coordination state of $Fe^{II}OEP$, being four-coordinate at low [py] and six-coordinate at high [py]. A similar interpretation of ligand-concentration-dependent $E_{1/2}$ shifts for $FeTPP(4MeImH)_2^+$ seems unlikely since the magnitude of the observed shift is significantly less than that predicted for coordination effects.[34] This conclusion is supported by the results of an analogous experiment with 1MeIm in place of 4MeImH. Solutions of 1 mM $FeTPP(1MeIm)_2SbF_6$ in either the presence or absence of 0.1 M 1MeIm give identical $E_{1/2}$ values for the Fe(III)/Fe(II) couple. That a shift is observed with 4MeImH and not 1MeIm implies an imidazole N–H is involved, suggesting that hydrogen bonding to coordinated 4MeImH is responsible for the observed shift. In any case, these results imply that reduction of **2** is not followed by ligand dissociation. Only one reducible

(29) Del Gaudio, J.; LaMar, G. N. *J. Am. Chem. Soc.* **1978**, *100*, 1112–1119 and references cited therein.

(30) Ainscough, E. W.; Addison, A. W.; Dolphin, D.; James, B. R. *J. Am. Chem. Soc.* **1978**, *100*, 7585–7591.

(31) Bottomley, L. A.; Kadish, K. M. *Inorg. Chem.* **1981**, *20*, 1348–1357.

(32) Lexa, D.; Momenteau, M.; Mispelter, J.; Lhoste, J. M. *Bioelectrochem. Bioenerg.* **1974**, *1*, 108–117.

(33) Kadish, K. M.; Bottomley, L. A. *Inorg. Chem.* **1980**, *19*, 832–836.

(34) Using $E_{1/2}$/log [L] = $0.059p/n$ where n = the number of electrons transferred, and p is the difference in the coordination number of Fe(III) and Fe(II), one would predict $E_{1/2}$/log [L] values of approximately 60 or 120 mV if Fe(II) is five- or four-coordinate, respectively.

and one reoxidizable species exist whether excess ligand is present or not. Hence, **2** must be fully ligated in both the ferric and ferrous states. Species **1**, on the other hand, undergoes partial ligand dissociation upon reduction, resulting in formation of some five-coordinate $Fe^{II}TPP(4MeIm)^-$. The fully formed, six-coordinate complex, $Fe^{II}TPP(4MeIm)_2^{2-}$ can thus only be observed in the presence of excess ligand. Relatively low ligand affinities of ferrous porphyrin imidazolate complexes have also been observed by other investigators.[11] In the present case, the large negative charge on the reduced six-coordinate complex may be responsible for the low affinity for the second imidazolate ligand.

Finally, comparison of $E_{1/2}$ of **2** and $^1/_2(E_{pc} + E_{pa})$ of **1** reveals that deprotonation results in an approximately 700-mV stabilization of the ferric state. Undoubtedly, a substantial portion of this effect is due to the charges of the species being reduced (i.e., **1** is an anion; **2** is a cation).

Acknowledgment. Financial support from the USPHS (Grant GM 28222 to J.S.V.), a BRSG grant (J.S.V.), and the NSF (C.E.S.) is gratefully acknowledged. R.Q. was the recipient of a Johnson and Johnson fellowship in chemistry administered by Rutgers University. We also thank Dr. C. Knobler and N. Keder for helpful discussions.

Registry No. **1**, 87494-49-3; $Fe(TPP)(4\text{-}MeImH)_2SbF_6$, 80939-26-0; $Fe(TPP)(SbF_6)$, 79949-97-6; Fe(TPP)Cl, 16456-81-8; Fe(TPP)(4-MeIm), 80925-73-1.

Supplementary Material Available: Calculated hydrogen atom positions (Table VIII), isotropic thermal parameters (Table IX), anisotropic thermal parameters (Table X), and a listing of observed and calculated structure factors (20 pages). Ordering information is given on any current masthead page.

Contribution from the Department of Chemistry and Materials and Molecular Research Division, Lawrence Berkeley Laboratory, University of California, Berkeley, California 94720

Specific Sequestering Agents for the Actinides. 9. Synthesis of Metal Complexes of 1-Hydroxy-2-pyridinone and the Crystal Structure of Tetrakis(1-oxy-2-pyridonato)aquothorium(IV) Dihydrate[1]

PAUL E. RILEY, KAMAL ABU-DARI,[2] and KENNETH N. RAYMOND*

Received April 1, 1983

The Zr(IV), Ce(IV), Th(IV), and U(IV) complexes of 1-oxy-2-pyridonate ($C_5H_4NO_2^-$) have been prepared, and the crystal structure of the dihydrate of the nine-coordinate complex $(C_5H_4NO_2)_4(H_2O)Th$ has been determined by single-crystal X-ray diffraction techniques with data obtained by counter methods. The Th(IV) complex consists of neutral molecules of rigorous C_2 symmetry in which Th(IV) and the coordinated water molecule lie along the C_2 axis parallel to *b*. The immediate coordination sphere about Th is completed by the eight oxygen atoms of the four bidentate $C_5H_4NO_2^-$ ligands [average r(Th–O) = 2.44 Å] and the water molecule [r(Th–O) = 2.52 Å], such that the resulting nine-coordinate complex resembles a D_{3h} tricapped trigonal prism, although the actual geometry is an intermediate nearly on the C_{2v} symmetry pathway between the C_{4v} monocapped Archimedean antiprism and the D_{3h} tricapped trigonal prism. The difference betweeen this structure and the similar nine-coordinate tetrakis(tropolonato)(*N*,*N*-dimethylformamide)thorium(IV) complex, which is closer to the C_{4v} structure, is explained as largely due to the asymmetric charge distribution in the oxypyridinone ligand as compared with tropolonate. The compound crystallizes as colorless parallelepipeds in the orthorhombic space group *Pbcn* with *a* = 12.880 (1) Å, *b* = 8.812 (2) Å, and *c* = 20.826 (2) Å. The calculated density (2.04 g cm^{-3}) agrees well with the measured value (2.04 g cm^{-3}) and is consistent with four formula units of the dihydrate per unit cell. Full-matrix least-squares refinement of the structure with use of the 2100 reflections with $F_o^2 > 3\sigma(F_o^2)$ has converged with R and R_w indices of 0.026.

Introduction

We have previously noted that the coordination chemistry of actinide(IV) ions is in some ways markedly similar to that of iron(III), and we have used this similarity to design highly specific actinide(IV) sequestering agents.[1,3] Incorporated into such synthetic macrochelating ligands have been those groups, principally catecholate and hydroxamate, that are known to bind iron(III) strongly in the bacterial iron transport and chelating agents called siderophores.

A detailed assessment of the architecture of the simple prototypical complexes formed between actinide(IV) ions and these small groups is particularly important if the desired synthetic macrochelating ligands are to be suitably designed to fulfill more satisfactorily—and hence more specifically—the coordination requirements of a particular actinide(IV) ion. Accordingly we have recently reported[3] the synthesis and the crystal structures of two eight-coordinate Th(IV) complexes of the bidentate hydroxamate ligands

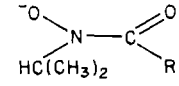

R = $CH_2C(CH_3)_3$, $C(CH_3)_3$

We have now extended this work by preparing metal complexes of the related bidentate ligand 1-oxy-2-pyridonate ($C_5H_4NO_2^-$)

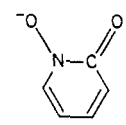

which in one view represents a slight variation of the common hydroxamate ligand depicted above and in another is iso-

* To whom correspondence should be addressed at the Department of Chemistry.

(1) Previous paper in this series: Abu-Dari, K.; Raymond, K. N. *Inorg. Chem.* **1982**, *21*, 1676.
(2) On leave from the Chemistry Department, University of Jordan, Amman, Jordan.
(3) Smith, W. L.; Raymond, K. N. *J. Am. Chem. Soc.* **1981**, *103*, 3341 and references therein.

0020-1669/83/1322-3940$01.50/0